

## INDUCTION MOTOR STATOR WINDING THERMAL PROCESS RESEARCH AND MODELLING UNDER LOCKED ROTOR MODE

Aleksejs Gedzurs, Andris Sniders

Latvia University of Agriculture, Faculty of Engineering, Institute of Agricultural Energetics  
aleksejs.gedzurs@inbox.lv, andris.sniders@llu.lv

**Abstract.** The paper discusses the transient heating process and response of a small-powered induction motor to extreme permanent overload-locked rotor under standard electrical supply system (400 V, 50 Hz) for cold initial conditions and constant ambient temperature. Experimental tests and analytical calculations, performed on a 1.1 kW totally enclosed fan-cooled three phase induction motor, show that stator windings heating is adiabatic with temperature dependent thermal losses and variable stator windings resistance, electrical current and power as the functions of the motor windings temperature. The transient temperatures are measured in 5 points of stator end windings, in 1 point of the motor casing and in 2 points of stalled cage rotor circuit using thermocouples, current sensors and loggers for data processing and archiving. To get an actual stator winding heating response to extreme overload (locked rotor) considering the dynamic error and different time constants of thermocouples, as a result of their thermal contact quality difference with the surface of stator windings, the simulations in MATLAB environment, using SIMULINK tools, are performed. The experimental tests, analytical calculations and simulations show that the stator winding heating curves obey the adiabatic thermal process with temperature growing rate  $4.8\text{ }^{\circ}\text{C}\cdot\text{s}^{-1}$ .

**Keywords:** induction motor, locked rotor, losses, stator windings, temperature, adiabatic heating.

### Introduction

The electric motor systems of all types and sizes account for 45 % of the electricity consumption in rotating machines totaling 7 600 PWh [1]. The largest proportion of motor electricity is attributable to mid-size electric motors with the output power of 0.75 kW to 375 kW. Many different electric motor technologies and design types are available, but induction motors are most frequently used and consume the most energy. Typical induction motor (IM) applications in rural industry include pumps, fans, compressors, mills, cranes, conveyors, crushers, etc. Statistics have shown that despite the IM high reliability and simplicity of construction, annual motor failure rate is conservatively estimated at 3-5 % per year, and in extreme cases, up to 12 % [2]. IM failures cause essential direct and technological losses involving motor change and repair, as well as interruption of the production process.

IM failures may be classified as follows: 1) electrical related failures  $\approx 35\%$ ; 2) mechanical related failures  $\approx 31\%$ ; 3) environmental impact and other reasons related failures  $\approx 34\%$  [2]. Other studies classify IM failures as follows – bearing faults  $\approx 40\%$ ; stator related  $\approx 38\%$ ; rotor related  $\approx 10\%$ ; other failures  $\approx 12\%$  [3]. The analysis of the IM failure reasons show that many of them are caused by prolonged heating of the different parts involved in IM operation. That is why an accurate tracking of IM thermal status and adequate response of the protection system to thermal overloads is important.

Detailed description of experimental and analytical research methods and results of the transient heating of IM parts and thermal modeling is given in [4-6]. The experimental investigations are performed on a low-power induction motor under stall, no-load, rated and overload conditions. If the thermal model is used in the IM design process, a fairly complex model is necessary, based on the numerical finite element method. If the thermal model is used for determining the heating of the existing IM parts, a simpler model can be used, often referred to as a thermal network model [4].

The most sensitive part of IM to thermal overloads is stator windings. Exceeding the temperature limit results in acceleration of the oxidation process in insulation materials what eventually leads to IM damage. The extreme mode of IM operation is locked rotor. Losses in stator windings are maximal, the rotation speed  $n = 0$ , the fan is out of order and heat dissipation from the windings area is minimal. The analysis of the electric motor failures show that 2 % of total stator related failures are caused by motor stall [3].

The objective of the study is to get experimental electrical and thermal parameters of the IM parts under locked rotor operation mode.

## Materials and methods

The heating process research has been performed in an electric drive laboratory on a three phase induction motor: 4AX80A4Y3; 220/380 V; 4.9/2.8 A; IP44; insulation class – B,  $m = 14.5$  kg;  $P = 1.1$  kW;  $n = 1400$  min<sup>-1</sup>;  $s = 0.67$ ;  $\eta = 0.75$ ;  $\cos\varphi = 0.81$ . The block diagram of the experimental setup for conducting tests is shown in Figure 1. The test bench is fitted with laboratory measuring equipment – voltmeters (V), ammeters (A) and watt meters (W) for monitoring of three phase current, voltage and power. For temperature measuring of IM stator casing and rotor and stator windings, eight miniature K-type thermocouples BK-50 (measurement error  $\pm 2.2$  °C) are installed. All thermocouples are connected to a data logger Pico-Log TC-08 with build in cold junction compensation (accuracy of temperature reading –  $\pm 0.2$  % and  $\pm 0.5$  °C). The stator frame surface temperature is measured by thermocouple  $T_6$ . Stator winding temperatures are measured for each phase (A, B, C) by five thermocouples ( $T_1, T_2, T_3, T_7, T_8$ ) attached to the end windings in the shaft and fan sides. The thermocouples are inserted into natural gaps in the end windings and bonded by thermal bandage. The temperature of the rotor is measured in the shaft side end rings by thermocouples  $T_4$  and  $T_5$ . For measuring of IM stator current and voltage current sensor (current clamps 3XTA011AC), voltage leads and data logger Simple Logger II L562 and Simple Logger L101 (accuracy – current  $\pm 0.5$  % of reading  $\pm 1$  mV, voltage –  $\pm 0.5$  % of reading  $\pm 1$  V) are used. To lock the rotor a mechanical coupling is used. All tests are performed under cold initial conditions – the initial temperature of IM parts is equal to the ambient temperature ( $\theta_0 = \theta_a$ ). The input voltage and frequency are uniform with the rated values (400 V, 50 Hz) in all phases. To simulate the heating process of the thermocouples and IM stator windings under locked rotor mode the MATLAB SIMULINK software is used.

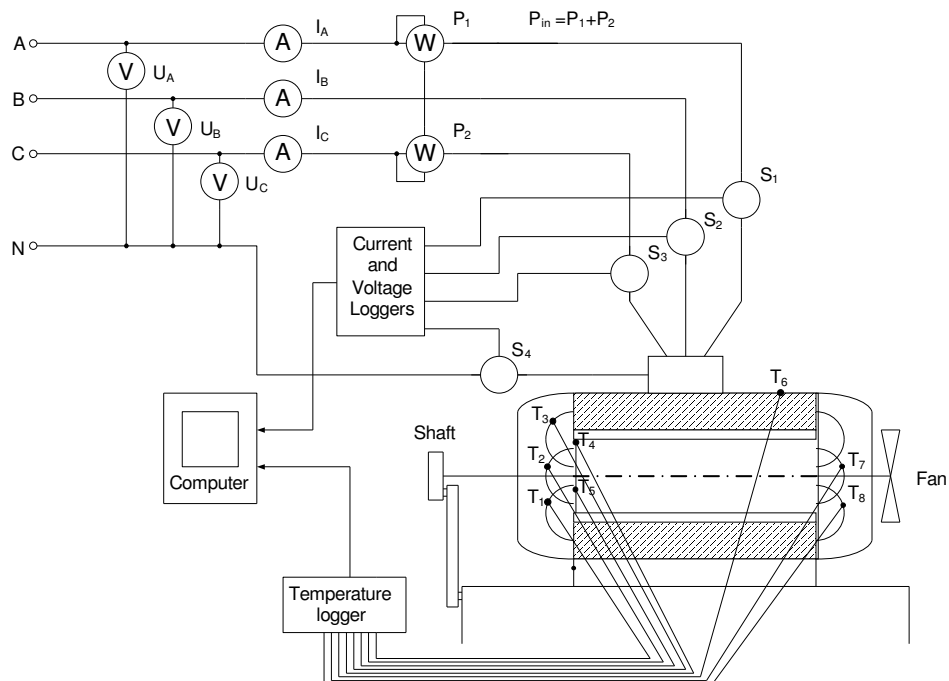


Fig. 1. Test bench set-up for induction motor heating experimental research under locked rotor:

$T_1, T_2, T_3, T_7, T_8$  – thermocouples (end windings – shaft and fan sides);  $T_4, T_5$  – thermocouple (rotor end rings shaft side);  $T_6$  – thermocouples (frame);  $S_1, S_2$  – current sensors;  $S_3, S_4$  – voltage leads

## Results and discussion

### IM heating response to permanent locked rotor overload

Figure 2 shows the IM thermal response to locked rotor overload. The initial temperature of IM all parts equal to the ambient temperature  $\theta_0 = \theta_a = 24$  °C. At the initial temperature 24 °C the measured stator winding resistance  $R_s = 7.4$   $\Omega$ , current  $I_s = 14.5$  A and active power  $P_{el} = 7320$  W. At the final temperature 157 °C –  $R_s = 11$   $\Omega$ ,  $I_s = 10.5$  A and  $P_{el} = 6120$  W. The calculated complex power at the initial temperature is  $S = 9570$  VA and  $S = 7110$  VA at the final temperature.

The stator end winding temperature rises with constant growing rate  $r_{\theta_s} = 4.8 \text{ }^\circ\text{C}\cdot\text{s}^{-1}$ . The stator winding temperature rises to  $157 \text{ }^\circ\text{C}$  at the switch-off point, rotor temperature –  $73 \text{ }^\circ\text{C}$ . The casing temperature during all operation period increases from the ambient temperature  $24 \text{ }^\circ\text{C}$  to  $27 \text{ }^\circ\text{C}$  at the winding temperature  $157 \text{ }^\circ\text{C}$ . The thermocouples in the end windings have different thermal time constants due to difference in the contact quality between the thermocouples and windings. The winding temperature  $\theta_{i2}$  at the switch-off point measured by the thermocouples with higher inertia is by  $15 \text{ }^\circ\text{C}$  less than temperature  $\theta_{i1}$  measured by the thermocouples with lower inertia. For regression analysis equations (1-3) are used to estimate the winding temperature, rotor temperature and current experimental data respectively.

$$\theta_i(t) = r_{\theta_i} \cdot t - r_{\theta_s} \cdot T_t \cdot (1 - e^{-\frac{t}{T_t}}) + \theta_a \tag{1}$$

where  $\theta_i$  – winding temperature measured by thermocouple,  $^\circ\text{C}$ ;  
 $\theta_a$  – ambient temperature,  $^\circ\text{C}$ ;  
 $T_t$  – thermal time constant of thermocouple, s;  
 $t$  – test run time, s;  
 $r_{\theta_s}$  – stator windings temperature growing rate,  $^\circ\text{C}\cdot\text{s}^{-1}$ .

$$\theta_r(t) = \Delta\theta_{r\max} \cdot (1 - e^{-\frac{t}{T}}) + \theta_a = \theta_{r\max} - \Delta\theta_{r\max} \cdot e^{-\frac{t}{T}} \tag{2}$$

where  $\theta_r$  – rotor temperature,  $^\circ\text{C}$ ;  
 $\theta_{r\max}$  – rotor steady state temperature,  $^\circ\text{C}$ ;  
 $\Delta\theta_{r\max} = \theta_{r\max} - \theta_a$  – maximum temperature raise of rotor,  $^\circ\text{C}$ ;  
 $T$  – thermal time constant, s.

$$I(t) = \frac{U}{\sqrt{(R_o + \Delta R(t))^2 + X^2}} \tag{3}$$

where  $I$  and  $U$  – current (A) and voltage, V;  
 $R_o$  and  $X$  – initial resistance and reactance,  $\Omega$ ;  
 $\Delta R$  – resistance change due to temperature raise,  $\Omega$ .

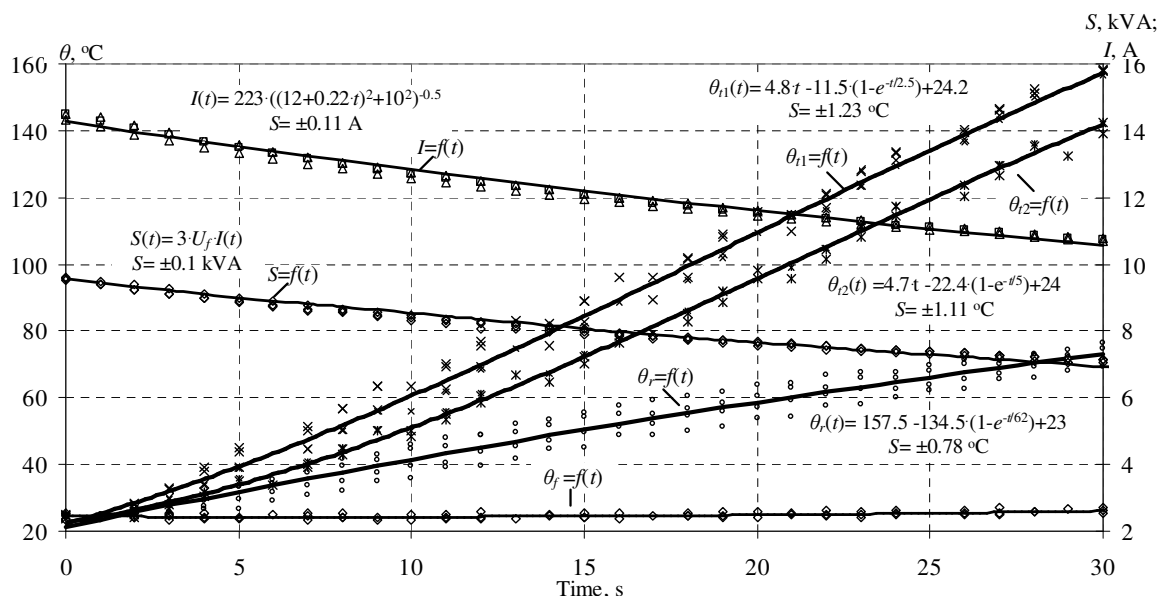


**Fig. 2. Response of induction motor part temperature under locked rotor mode:**  
 $\theta_{i1}(t)$  – temperature of stator end windings – shaft side,  $^\circ\text{C}$ ;  $\theta_{i2}(t)$  – temperature of stator end windings – fan side,  $^\circ\text{C}$ ;  $\theta_r(t)$  – temperature of rotor,  $^\circ\text{C}$ ;  $\theta_c(t)$  – casing temperature,  $^\circ\text{C}$ ;  
 $S(t)$  – complex power, kVA;  $I_s(t)$  – stator current, A

### IM short-circuit locked rotor operation and zero speed testing

If the load torque of IM exceeds the critical value, the rotor stays at a standstill mode. Losses in stator windings are maximal, the rotation speed  $n = 0$  and slip  $s = 1$ , the fan is out of order and heat dissipation from windings is practically zero during all along temperature rise to the critical value of the insulation thermal class. The heating process is adiabatic.

For frequencies 50/60 Hz and prolonged rotor stall only stator and rotor winding losses are considered, because of very small losses in the core [7]. Therefore, all input electrical power transforms to heat losses in IM stator and rotor electrical circuits. On the bases of the experimental research results the single phase equivalent circuit of IM for long time locked rotor conditions has been composed (Fig.3).

Summary electrical losses in stator and rotor equivalent circuit are calculated using the experimental research data:

$$P_{el} = P_s + P_r \approx 3I_s^2 R_s + 3I_r'^2 R_r' \approx 3I_s^2 (R_s + R_r'), \quad (4)$$

where  $P_{el}$  – measured electrical input power at given stator windings temperature, W;  
 $P_s$  and  $P_r'$  – calculated stator and rotor losses, related to stator circuit, W;  
 $I_s$  and  $R_s$  – measured stator current (A) and stator resistance,  $\Omega$ ;  
 $I_r' = I_s$  – rotor current related to stator circuit, A;  
 $R_r'$  – calculated resistance of rotor, related to stator circuit,  $\Omega$ .

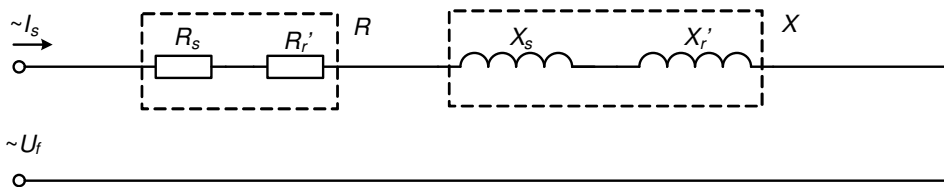


Fig. 3. Equivalent electrical circuit of induction motor for single phase under long time rotor stall:  $U_f$  – single phase voltage, V;  $I_s$  – stator current, A;  $R_s$  and  $X_s$  – stator resistance and reactance,  $\Omega$ ;  $R_r'$  and  $X_r'$  – rotor resistance and reactance related to stator circuit,  $\Omega$

With  $U_f$ ,  $P_{el}$ ,  $I_s$  and  $R_s$  measured, the resistance  $R_r'$  and reactance of equivalent circuit  $X = X_s + X_r'$  may be calculated:

$$R_r' \approx \frac{P_{el}}{3I_s^2} - R_s, X = \sqrt{\frac{U_f^2}{I_s^2} - (R_s - R_r')^2}. \quad (5)$$

The calculated  $R_r'$  and  $X$  (formula 5) for initial conditions - stator windings temperature equals to ambient temperature ( $\theta_s = \theta_a = 24^\circ\text{C}$ ) and measured  $U_f = 223$  V,  $P_{el}(24^\circ\text{C}) = 7320$  W,  $I_s(24^\circ\text{C}) = 14.5$  A,  $R_s(24^\circ\text{C}) = 7.4$   $\Omega$ , are as follows:  $R_r'(24^\circ\text{C}) = 4.2$   $\Omega$  and  $X(24^\circ\text{C}) = 10$   $\Omega$ . The calculated stator losses  $P_s$  and rotor losses  $P_r'$  (formula 1) for initial conditions ( $\theta_s = \theta_a = 24^\circ\text{C}$ ) are as follows:  $P_s(24^\circ\text{C}) = 4670$  W and  $P_r'(24^\circ\text{C}) = 2650$  W.

For the final conditions ( $\theta_s = 157^\circ\text{C}$ ) and measured  $U_f = 223$  V,  $P_{el}(157^\circ\text{C}) = 6120$  W,  $I_s(157^\circ\text{C}) = 10.5$  A,  $R_s(157^\circ\text{C}) = 11$   $\Omega$ , the calculated  $R_r'$  and  $X$  (formula 2) are as follows:  $R_r'(157^\circ\text{C}) = 7.5$   $\Omega$  and  $X(157^\circ\text{C}) = 10$   $\Omega$ . The calculated stator losses  $P_s$  and rotor losses  $P_r'$  (formula 1) for final conditions ( $\theta_s = 157^\circ\text{C}$ ) are as follows:  $P_s(157^\circ\text{C}) = 3640$  W and  $P_r'(157^\circ\text{C}) = 2480$  W.

The calculations show that the reactance  $X$  stays constant, but electrical losses in the stator circuit slowly decrease for 22 % with temperature rise from  $24^\circ\text{C}$  to the maximum value –  $157^\circ\text{C}$ .

Heat transfer from the stator windings to the thermocouple may be described by the following algorithms:

$$T_t \frac{d\Delta\theta_t}{dt} + \Delta\theta_t = \Delta\theta_s, T_t \cdot \Delta\theta_t(s) \cdot s + \Delta\theta_t(s) = \Delta\theta_s(s), W(s) = \frac{\Delta\theta(s)}{\Delta\theta(s)} = \frac{1}{T_t \cdot s + 1}, \quad (6)$$

where  $\Delta\theta_t$  – thermocouple temperature rise,  $^\circ\text{C}$ ;  
 $\Delta\theta_s$  – stator windings temperature rise,  $^\circ\text{C}$ ;

$\Delta\theta_i(s)$  – Laplace transform of thermocouple temperature rise, °C;  
 $\Delta\theta_s(s)$  – Laplace transform of stator temperature rise, °C;  
 $W(s)$  – transfer function of thermocouple;  
 $s$  – Laplace variable,  $s^{-1}$ .

**The model of IM stator winding temperature measurement in SIMULINK**

For the IM stator winding adiabatic heating process research and for temperature measurement accuracy estimation to take into account the temperature growing rate, the physical parameters of the temperature sensors – thermocouples, as well as their installation quality, what largely estimates an accuracy of temperature testing, the simulation block diagram of IM stator winding temperature measurement in MATLAB SIMULINK environment has been compiled (Fig. 4).

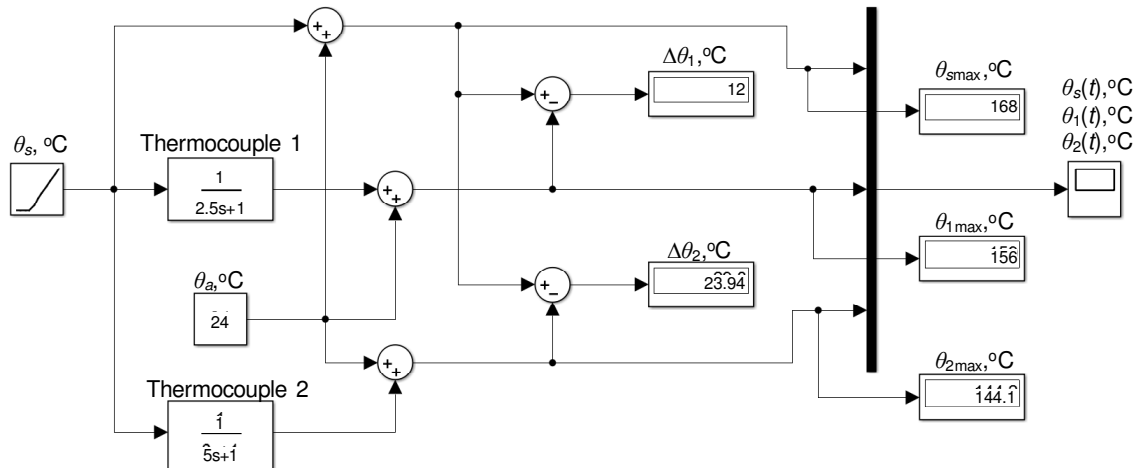


**Fig. 4. Simulation block diagram of IM stator windings temperature measurement under long time rotor stall:**  $\theta_s$  – linear growing temperature of stator end windings, °C;  $\theta_a$  – ambient (initial) temperature of stator end windings, °C;  $\theta_1, \theta_2$  – temperature rise of stator end windings measured by virtual thermocouples (1 and 2) with time constants ( $T_1 = 2.5$  s,  $T_2 = 5$  s), °C;  $\Delta\theta_1, \Delta\theta_2$  – steady-state error of stator windings temperature measurement, °C

Simulated response of IM stator windings and two virtual thermocouples with time constants  $T_1 = 2.5$  s and  $T_2 = 5$  s to adiabatic heating process is shown in Figure 5. After transient time, caused by virtual thermocouple reaction delay, temperature rises gradually with constant growing rate  $r_{\theta_s} = 4.8$  °C · s<sup>-1</sup>. Steady error of temperature virtual measuring by thermocouple T1 –  $\Delta\theta_1 = r_{\theta_s} \cdot T_1 = 4.8 \cdot 2.5 = 12$  °C. Steady error of virtual thermocouple T2 is two times greater, because of proportionally higher time constant –  $\Delta\theta_2 = r_{\theta_s} \cdot T_2 = 4.8 \cdot 5 = 24$  °C.

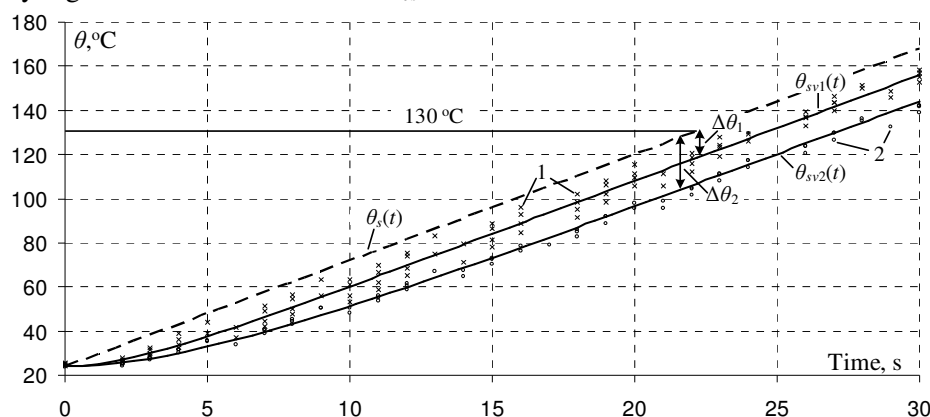


**Fig. 5. Simulated response of IM stator winding temperature to locked rotor mode:**  $\theta_s(t)$  – actual temperature rise of stator end windings, °C;  $\theta_{sv1}, \theta_{sv2}$  – temperature rise of stator end windings measured by virtual thermocouples with time constants  $T_1 = 2.5$  s,  $T_2 = 5$  s, °C; 1, 2 – measured temperature rise of stator end windings by physical thermocouples, °C;  $\Delta\theta_1, \Delta\theta_2$  – simulated steady-state error of stator windings temperature rise, °C

The simulated temperature of stator end windings  $\theta_s(t)$  rises linear with constant growing rate  $r_{\theta_s} = 4.8 \text{ }^\circ\text{C}\cdot\text{s}^{-1}$  without reaction delay. To obtain accurate physical measuring data of IM stator winding temperature high-speed rise, the thermal time constant of the temperature sensor should be equal to zero, what is practically impossible. The model parameters and simulated curves  $\theta_{sv1}(t)$  and  $\theta_{sv2}(t)$  of the virtual thermocouples are harmonized with the experimental data 1 and 2 (Fig. 5.)

### Conclusions

1. The experimental tests show that under locked rotor operation IM stator end winding temperature  $\theta_s$  growing rate is  $4.8 \text{ }^\circ\text{C}\cdot\text{s}^{-1}$  and the thermal limit for B insulation class –  $130 \text{ }^\circ\text{C}$  reaches in 21 seconds, while the case temperature practically stays constant, what means that under locked rotor the IM stator winding heating process is adiabatic up to insulation thermal limit temperature.
2. The different thermocouple thermal time constants are due to the contact quality between the thermocouple and windings. It shows that during a fast heating process response delay of the temperature sensors plays an essential role to measure the actual temperature of an object with appropriate accuracy.
3. The experimental data and simulation results show that the thermocouple heating process may be represented as a first order inertial model described by differential equation with a constant thermal parameter - heating time constant  $T$  dependent on the thermocouple physical parameters and installation quality in the control object. Dynamic error of IM winding temperature measurement for the adiabatic process increases in proportion with the time constant of the temperature control sensor.
4. The simulation results of IM stator winding heating under locked rotor conditions show that steady-state error of the end winding temperature measurement increases in proportion with the temperature growing rate  $r_{\theta_s}$  and with the thermal time constant  $T$  of the temperature sensor. To predict in time the moment of IM switching off under extreme mechanical overload – stalled rotor the temperature protective device of IM should be adaptive to the temperature growing rate and to response delay of the temperature sensor.

### References

1. Brunner C.U., Werle R. Market Transformation Program for Electric Motor Systems: Global progress report and outlook, 4E EMSA, Zurich, Austria, 2013, 16 p.
2. Venkataraman B., Godsey B., Premerlani W., Shulman E.etc. Fundamentals of a Motor Thermal Model and its Applications in Motor Protection. In: Proceedings of 58<sup>th</sup> Annual Conference “Protective Relay Engineers”, Black & Veatch Corporation, Kansas City, USA, 2005, pp. 127-144.
3. Thurston M.O. Handbook of Electric Motors. CRC Press, Boca Raton, USA, 2004, 773 p.
4. Kylander G. Thermal Modeling of Small Cage Induction Motors: Technical Report No. 265, Goteborg, Sweden, Chalmers University of Technology, 1995.-113 p.
5. Sniders A., Gedzurs A. Non-stationary Heating of Low-power Induction motor Under Continued Overload. In: Proceedings of 11<sup>th</sup> International Scientific Conference “Engineering for Rural Development”, Latvia University of Agriculture, Jelgava, Latvia, 2012, pp. 536-542.
6. Zhang P. Active Thermal Protection for Induction Motors Fed by Motor Control Devices: Dissertation, Georgia Institute of Technology, Georgia, USA, 180 p.
7. Boldea I., Nasar S.A. Induction Machines Design Handbook. CRC Press, Boca Raton, USA, 2010, 824 p.